福井大学
工学部 研究報告
第47巻 第1号
1999年3月

Basic Design of UV Rotational Raman Lidar for Temperature Measurement of the Troposphere

Dongsong SUN* and Takao KOBAYASHI*

(Received Feb. 26, 1999)

Basic analysis of practical rotational Raman lidar (laser radar) system for the temperature measurement of the troposphere is presented. The eye-safe UV laser of 355nm wavelength is selected as the transmitter and anti-Stokes lines of the rotational Raman backscatter are used for the temperature determination. From the system design, it is concluded that the temperature accuracy of 1K can be obtained up to 10km height with 5W average laser system.

Key Words : Lidar, Rotational Raman Scatter, Temperature, UV Lidar, Troposphere

1. Introduction

The advantageous features of laser remote probing techniques have attracted much attention and led to the development of lidars or laser radars for measuring various atmospheric parameters such as composition, optical properties, and meteorological condition. A variety of interaction phenomena accompanying laser light propagation through the atmosphere makes it possible to obtain information about the meteorological parameters, i.e., temperature, humidity, and wind speed. Temperature is one of the basic atmospheric parameters and global measurements are required in essentially all weather for climate prediction. There has been an extensive radiosonde network in the globe established to meet this need. The problem to be solved, however, is the resolution of altitude and accuracy. The vertical temperature of current sondes is limited to 5 to 8 km with the limitations in temperature accuracy to ~2K[1]. In the past, four lidar techniques have been investigated to obtain improved measurements of the atmospheric temperature, i.e., the two-wavelength differential absorption lidar (DIAL)[2]; the Rayleigh molecular density method[3]; the Rayleigh spectral width method[4]; and the rotational Raman scatter method[5]. However, none of these systems have been used as practical and reliable sensing systems for the temperature measurement of the troposphere.

The rotational Raman method was first suggested by Cooney[5]. The temperature accuracy of 4K was obtained at the low altitude. In recent decade, the temperature profile by this method has been extended from troposphere to stratosphere[6] using the visible lasers of 532nm wavelength

* Dept. of Electrical and Electronic Engineering

with the results of reasonably good agreement with sonde measurements. As the Mie and Rayleigh elastic backscatter must be eliminated in this method, high rejection and efficient filters are required.

In this paper we will compare and optimize the sensitivity of the rotational Raman lidar and show that UV wavelength is superior for the lidar system. The principle and basic design of the rotational Raman lidar for practical and operational temperature measurement are presented together with the simulation results of the sensitivity of the Raman lidar system.

2. Principle of temperature measurement with rotational Raman backscatter

The rotational Raman spectrum contains two side-bands, O (anti-Stokes) and S (Stokes) branches of approximately equal amplitude. These branches are positioned spectrally symmetrically on both side of the exciting line. The intensity of rotational Raman backscatter line is given by[7]

$$I = N_0 I_0 F_J (d\sigma/d\Omega), \tag{1}$$

where I_0 is the laser intensity of incident beam, N_0 is the number density of atmospheric molecules under study, F_J is the rotational fraction of molecules in the rotational quantum state J, $d\sigma/d\Omega$ is the rotational differential cross section from the state J to J', and β_{Ram} is the volume backscattering coefficient given by $\beta_{Ram}=N_0F_J(d\sigma/d\Omega)$. An approximate expression for F_J for a gas in thermal equilibrium at a temperature T is

$$F_J = g_J \frac{2J+1}{(2I+1)^2} \frac{2hcB}{kT} e^{-\frac{Bhc}{kT}J(J+1)}, \tag{2}$$

where g_J is a statistical weight factor (equal to 6 and 3 for even and odd N_2 lines, and 0 and 1 for

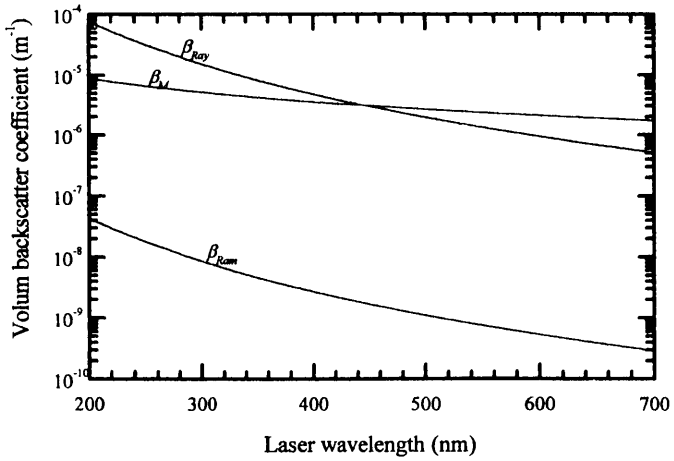

Fig.1 Volume backscatter coefficients of Raman anti-Stokes line (J=6), Rayleigh and Mie backscatter as a function of laser wavelength. The US atmosphere standard is used.

even and odd O_2 lines, respectively), I is the nuclear-spin quantum number (1 for N_2, 0 for O_2), B is the molecular rotational constant (1.98973cm^{-1} for N_2 and 1.4378cm^{-1} for O_2). The differential cross section for anti-Stokes Raman line is expressed as

$$\frac{d\sigma}{d\Omega}=\frac{64\pi^4}{45}\frac{3J(J-1)}{2(2J+1)(2J-1)}(\omega_0+\Delta\omega)^4\gamma^2, \tag{3}$$

where γ is the anisotropy of the molecular-polarizability tensor (0.518×10^{-48}cm^6 for N_2, and 1.35×10^{-48}cm^6 for O_2). $\Delta\omega$ is the Raman shift, which is $(4J\text{-}2)B$ for anti-Stokes line.

The volume backscattering coefficients of Raman rotational scatter and Rayleigh scattering for 355nm laser wavelength are plotted for the air molecules of N_2 and O_2 in **Fig.1**. The backscatter coefficient of anti-Stokes line (J=6) of Raman backscatter is more than 3 order smaller than that of the Rayleigh backscatter. So the rejection of 10^5 is required for the practical measurement with the signal-to-noise ratio of 10^2. In UV wavelength, the Mie backscatter is smaller than the Rayleigh backscatter. But in visible wavelength, the Mie backscatter is strong and the rejection is required higher than 10^6. On the other hand, with the altitude increasing the Mie backscatter can be neglected, the rejection for different wavelength is almost same because the ratio of the Raman backscatter to the Rayleigh backscatter becomes constant.

The rotational Raman backscatter spectrum is calculated and plotted in **Fig.2**. As the backscatter intensities of the rotational Raman lines are temperature dependent, the ratio of the two selected line intensities of Stokes or anti-Stokes lines can be used for temperature determination. For anti-Stokes lines, the ratio from Eq.(1) is given by

$$R(T)=\frac{J_1(J_1-1)(2J_2-1)}{J_2(J_2-1)(2J_1-1)}\left(\frac{\omega_0+\Delta\omega_1}{\omega_0+\Delta\omega_2}\right)^4 e^{-\frac{Bhc}{kT}[J_1(J_1+1)-J_2(J_2+1)]} \tag{4}$$

where J_1 and J_2 are the quantum numbers of these two lines respectively. The change of β_{Ram} for 1K temperature is defined as the temperature coefficient expressed as

$$\theta_T=\frac{d\beta_{Ram}}{dT}=\beta_{Ram}\frac{Bhc}{kT^2}[J(J+1)]. \tag{5}$$

In the low temperature, the temperature coefficient increases. The coefficient for N_2 molecule is higher than that of O_2. The normalized temperature sensitivity θ_T is shown in **Fig.3**. It can be seen

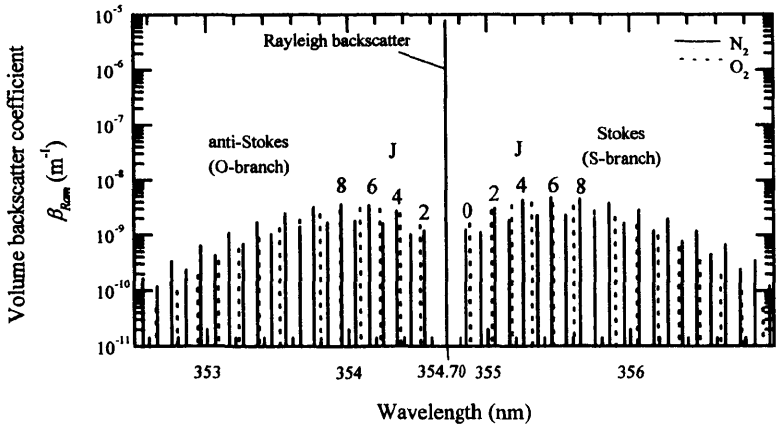

Fig.2 The spectrum of volume backscattering coefficient of the rotational Raman lines and the Rayleigh line for the atmospheric N_2 and O_2 molecules at 300K with the incident laser wavelength of 354.7nm.

that the absolute values of coefficients of anti-Stokes lines 4, 6, 14 and 16 are relatively high. But the volume backscatter coefficient is low for the large quantum number. In practical measurement, two filters (filter-1 and filter-2) are located at the lines of J_1 and J_2 and several rotational lines of N_2 and O_2 molecules are detected because of filter width. The difference of the volume backscatter coefficients for these two lines varying with unity temperature change can be defined as the temperature sensitivity γ, which is related to the temperature measurement accuracy, given by

$$\gamma = \frac{d}{dT}[\beta_{Ram}(J_1) - \beta_{Ram}(J_2)]. \tag{6}$$

Figure 4 shows the temperature sensitivity with the selection of two lines J_1 and J_2. The sensitivity of Stokes lines is little higher than that of anti-Stokes lines for the same J_1. The optimum line pairs are (4, 14) and (6, 14) for Stokes and anti-Stokes. Considering the rejection of elastic backscatter, the reasonable selection will be (6, 14) line pair.

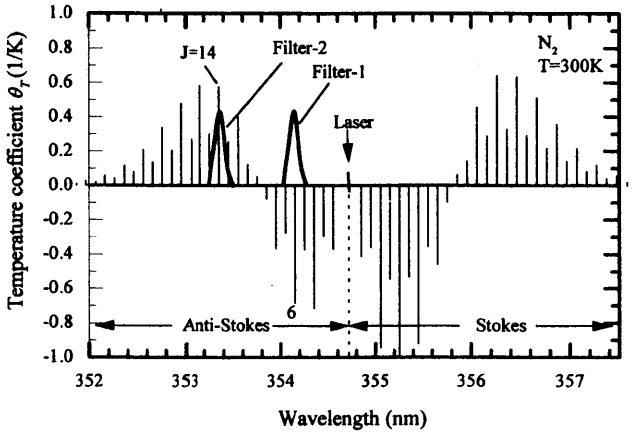

Fig.3. Temperature coefficient of rotational Raman lines as a function of the quantum number for N_2 at the temperature of 300K.

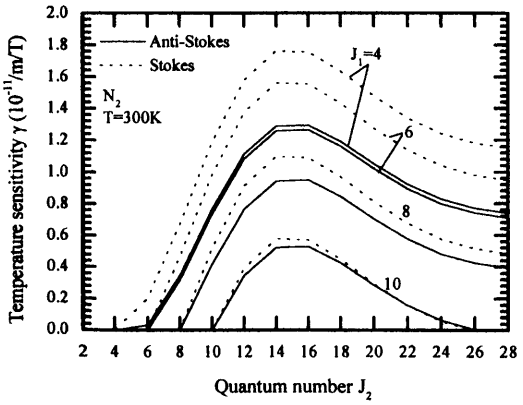

Fig.4 Variation of the temperature sensitivity with the quantum number J_1 and J_2 for Stokes and anti-Stokes lines of N_2 molecule.

3. Rotational Raman lidar system

Since the rotational Raman lines are very close to the intense Mie and Rayleigh backscatter, high rejection filters are necessary[8]. Because the Stokes lines may contain the fluorescence noise depending on the aerosol species[9], the anti-Stokes line is preferable for the temperature measurement. Narrow bandwidth filters are also necessary for daytime measurement to reject the background noise. The double path diffraction grating is expected for the Raman lidar system.

The diagram of the rotational Raman lidar system is shown in **Fig.5**. The designed parameters of the lidar system are given in **Table 1**. The system uses the Nd:YAG laser, frequency tripled beam at 355nm with 20Hz repetition and 1W average power. The backscatter light is collected by the telescope with a diameter of 250mm. The two gratings used in series can separate the Mie and anti-Stokes line (J=6) by about 0.5mm. Two pinholes are placed at the focus plane after the second grating for the two-channel detection. The photomultipliers with photon counters receive the scattered light.

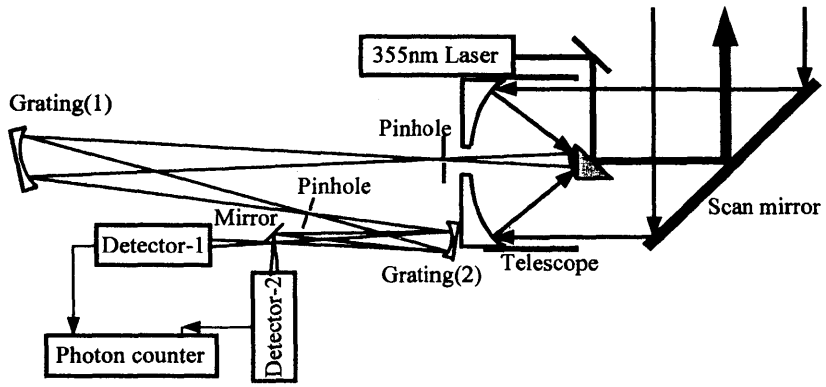

Fig.5. Schematic of the UV rotational Raman lidar for temperature profiling of the troposphere.

Table 1. System parameters of the Rotational Raman lidar

Laser: Nd:YAG		Detector: PMT Photon counting	
Wavelength (λ)	354.7nm	Quantum efficiency (η)	30%
Energy per pulse (E)	50mJ, (5mJ)	Dark current	1nA
PRF	20Hz, (1kHz)	Solar irradiance[10]	1.183W/m^2/nm
Optics:		Grating:	
Telescope diameter	250mm	Bandpass $\Delta\lambda$	0.4nm
FOV	0.1mrad	Groove density	2400gr/mm (1st)
Total transmission (T)	0.2		1200gr/mm(2nd)

The number of received photo-electrons is given by the well-known lidar equation

$$n = \frac{\eta E \lambda}{hc} Y(R) \beta_{Ram} \Delta R \frac{A}{R^2} T_{atm}^2 T_{sys} \tag{7}$$

and

$$\beta_{Ram} = \sum_J \left\{ N(N_2)\, d\sigma(\lambda_J)/d\Omega\big|_{N_2} + N(O_2)\, d\sigma(\lambda_J)/d\Omega\big|_{O_2} \right\} \cdot f(\lambda) \tag{8}$$

where $Y(R)$ is the overlap function of the telescope, β_{Ram} is the backscatter coefficient of the Raman backscatter, $N(N_2)$ and $N(O_2)$ are number density of atmospheric molecule N_2 and O_2; respectively, $f(\lambda)$ is the filter transmission function.

Assuming that the Mie and Rayleigh backscatter is blocked or much low comparing with the Raman backscatter, the signal-to-noise ratio is expressed as

$$\frac{S}{N} = \frac{\sqrt{mn}}{\sqrt{n + n_b + n_d}}, \tag{9}$$

where m is the laser pulse accumulation number, n_b is the number of background photo-electrons, n_d is the number of the dark current electrons. In the daytime the background intensity can be considered to be $0.34I_0(\lambda)/\pi$[11], where $I_0(\lambda)$ is the solar irradiance at the top of the atmosphere. The evaluated error ε of temperature measurement can be calculated by

$$\varepsilon = \frac{1}{(S/N)\cdot\theta_T}, \tag{10}$$

where S/N is the signal-to-noise ratio for the measurements of the atmospheric backscattered signals from two channel detectors. The anti-Stokes line pair of (6,14) is chosen for the temperature measurements according to the discussion in Section 2 at the wavelength 353.92nm and 353.32nm. From the Eqs.(4) and (6), the temperature can be deduced by the ratio of received photons for these anti-Stokes lines expressed by

$$\frac{n(\lambda_1)}{n(\lambda_2)} = \frac{\sum[F_J\beta(N_2) + F_J\beta(N_2)]f(\lambda_1)}{\sum[F_J\beta(N_2) + F_J\beta(N_2)]f(\lambda_2)} = ae^{\frac{b}{T}}. \tag{11}$$

If the filter bandwidth is designed to be 0.4nm and 0.6nm, a and b are constants given as theoretically 0.338 and 344.5, respectively. In the practical experiment, the values of a and b are experimentally decided for the system.

4. Numerical results of system sensitivity and discussion

From Eqs.(5), (8) and (10), the temperature measurement error is calculated. In **Fig.6**, the temperature error and filter width relation is compared at the height of 1km. The spectral centers of filter-1 and filter-2 are chosen with the line pair of J_1=6 and J_2=14, the filter-2 width is preliminarily selected by minimizing the temperature error. Considering that the output of the 2nd harmonic of Nd:YAG laser is two times higher than that of the 355nm 3rd harmonic, the laser energy of 532nm wavelength is selected to be 100mJ and 50mJ, respectively. The filter width for 532nm is selected wider than that for 355nm, because the Raman wavelength shift is large at longer wavelengths. For the night measurement, the minimum temperature error for 532nm wavelength is little larger than that of 355nm wavelength. The optimum width of filter-1 can also be found.

The temperature error of the lidar system with the system parameters of Table 1 is calculated in **Fig.7**. The temperature accuracy of 2K can be obtained up to about 8km height with our laboratory system. It shows the accuracy of 1K at 10km height with the advanced system of the average laser power of 5W (laser energy of 5mJ and the PRF of 1kHz). As the temperature

coefficient increases in lower temperature, the measurement error for high altitude will be less than the value shown in Fig.7, because the temperature generally decreases with height.

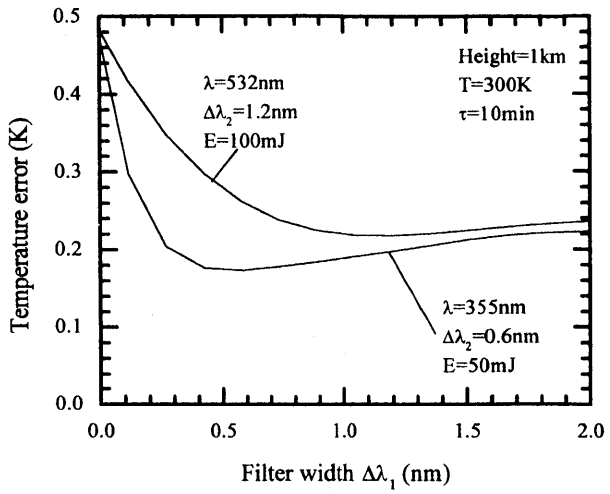

Fig.6 Change of temperature accuracy with filter width $\Delta\lambda$ for 355nm and 532nm wavelength at 1km height for J_1=6 and J_2=14 line pairs.

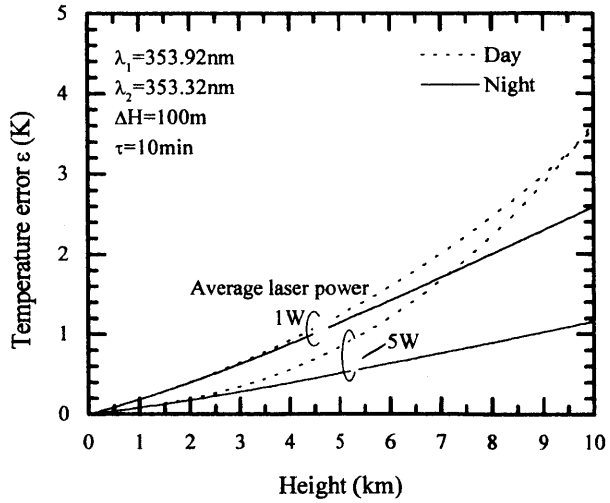

Fig.7 Temperature accuracy versus height relation for the night and daytime measurement. The two anti-Stokes lines of J_1=6 and J_2=14 are detected.

5. Conclusion

A rotational Raman lidar for tropospheric temperature measurement is proposed and evaluated. The UV 355nm laser can be used in the system because of high temperature accuracy comparing with that of the visible laser and eye-safety characteristics. The temperature accuracy is

discussed for optimizing the filter position. The filter spectral parameters are discussed. Two gratings are used in the system to get the rejection of more than 10^5 for Mie and Rayleigh backscatter. From previous experiments of rotational Raman lidar, the anti-Stokes line is suggested in the measurement. The temperature error of 2K can be obtained up to 8km with the laser of 1W average power. With the laser of 5W average power for 10 minute observation time, it is expected that the accuracy of 1K can be attained up to 10km height.

References

(1) L.D. Kaplan, M.T. Chahine, J. Susskind and J.E. Searl, "Spectral band passes for a high precision satellite sounder", *App. Opt.*, **16**, 322 (1977).

(2) C.L. Korb, G.K. Schwemmer, J. Famiglietti, H. Walden and C. Prasad, "Differential absorption lidars for remote sensing of atmospheric pressure and temperature profiles," Final Report, *NASA Technical Memorandum,* **104618**, 1995.

(3) G.S. Kent and R.W. Wright, "A review of laser radar measurements of atmospheric properties", *J. Atmos. Terr. Phys.*, **32**, 917(1970).

(4) C.A. Tepley, S.I. Sargoytchev and R. Rojas, "The Doppler Rayleigh Lidar Systems at Arecibo", IEEE Trans. On Geos. & Rem. Sens., **31**, 36(1993).

(5) J.A. Cooney, "Measurement of atmospheric temperature profiles by Raman backscatter", *J. Appl. Meteorol.*, **11**, 108(1972).

(6) D. Nedeljkovic, A. Hauchecorne and M.L. Chainin, "Rotational Raman Lidar to Measure the Atmospheric Temperature form the Ground to 30km", *IEEE Tran. Geosci. Remote Sensing,* **31**, 90(1993).

(7) C.M. Penney, R.L. St.Peters and M. Lapp, "Absolute rotational Raman cross sections for N_2, O_2, and CO_2", *J.O.S.A.*, **64**, 712(1974).

(8) T. Yamamoto, T. Taira and T. Kobayashi, "Development of a Rotational Raman Laser Radar for Remote Atmospheric Temperature Profiling", *Research Report of Faculty of Engineering, Fukui University*, **41**, 49(1993).

(9) T. Kitada, A. Hori, T. Taira and T. Kobayashi, "Strange Behavier of the Measurement of Atmospheric Temperature Profiles of the Rotational Raman Lidar", *17th Conference on Laser Atmospheric Studies*, Sendai, Japan, 567(1994).

(10) M.P. Thekaekara, "Extraterrestrial Solar Spectrum, 3000–6100 $\mathring{A}$ at 1-$\mathring{A}$ Intervals", *App. Opt.*, **13**, 518(1974).

(11) J.D. Spinhirne, "Micro Pulse Lidar", *IEEE Trans. on Geosci. & Remote Sensing*, **31**, 48(1993).